Équations aux dérivées partielles et leurs applications
Actes du colloque Edp-Normandie. Le Havre 2015. 185–195.
FNM Fédération Normandie Mathématiques

Considerations for the Finite Element Approximation of Three-Dimensional Domains*

Fleurianne Bertrand†

Abstract. During our study of first-order system least squares methods on domains with curved boundaries we needed to consider the three-dimensional case more precisely. A procedure for the construction of the domain and of the parametric mapping to retain the convergence order is presented. ©EDP-Normandie. All rights reserved.

Keywords. First-order system least squares; Parametric elements; Interpolation; Curved boundaries.

1. Introduction

This paper is a note on the construction of finite element approximation of three-dimensional domains that appear during the investigation of the finite element approximation on curved boundaries using Raviart-Thomas spaces in the context of first-order system least squares methods. In [1] it is shown that using a polygonal approximation of the boundary leads to an optimal order of convergence in the lowest-order case. Further, the authors demonstrate by numerical experiments that it is not sufficient in the higher-order case. To retain the optimal convergence order for the first-order system least squares approach in the higher-order case, we combine (see [2]) isoparametric finite elements of degree $k+1,\ k \geqslant 1$ for the scalar variable with parametric Raviart-Thomas spaces of degree k.

Therefore, a detailed treatment of curved boundaries in the context of face-based finite elements where Neumann boundary conditions are imposed on the normal flux is needed. The issue of parametric face-based elements has recently received attention in connection to exact sequences of finite element spaces (see e.g. [5]). A framework for the implementation of parametric Raviart-Thomas elements is provided in [6], although its motivation differs and it focuses on the case of an affine mapping.

The main contribution of this paper is to present the procedure (see [4]) for the construction of an approximated domain Ω_h with piecewise polynomial boundary Γ_h and of the mapping between this domains and the exact one, such that the convergence order is retained.

* Submitted : September 25, 2015. Accepted (in revised form) : December 22, 2015.
†Fakultät für Mathematik, Universität Duisburg-Essen, Germany.
fleurianne.bertrand@uni-due.de

In this paper, a bounded domain $\Omega \subset \mathbb{R}^3$ with a piecewise C^{k+2} and Lipschitz continuous boundary Γ is considered. We will present a procedure to cover Ω completely by a triangulation $\widetilde{\mathcal{T}}_h$, that needs to admit curved tetrahedrons adjacent to the boundary Γ, in general.

2. Construction of the Approximated Domain

The first step of the construction of the approximated domain is the interpolation of the boundary. Therefore, let $\boldsymbol{\gamma}\ :\ D \subset \mathbb{R}^2 \to \mathbb{R}^3$ denote a parametrization of Γ such that

$$\Gamma = \{\boldsymbol{\gamma}(\mathbf{x})\ :\ \mathbf{x} \in D\}\ . \tag{2.1}$$

$D \subset \mathbb{R}^2$ implies that it can be triangulated by a triangulation $\mathcal{S}_h$ such that

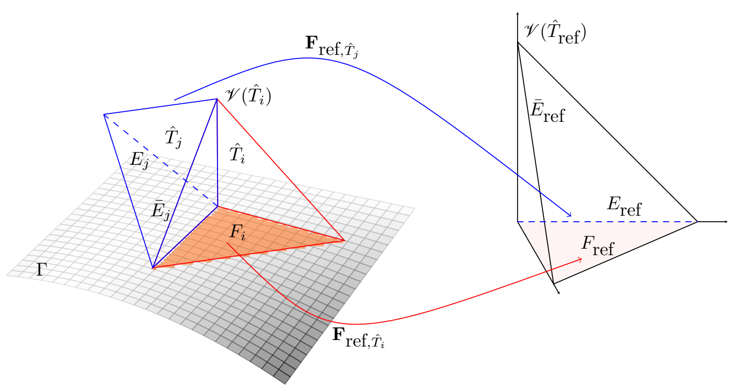

Fig. 2.1. *The intersection of $\hat{\Gamma}$ with $\hat{T}$ is a face (case $\hat{T}_i$) or an edge (case $\hat{T}_j$)*

1. $\{\mathcal{S}_{h,p_i}\}_{i=1}^{N_P}$ denotes the set of vertices in $\mathcal{S}_h$.
2. The polygon $\hat{\Omega}$ formed with all the vertices $\{\boldsymbol{\gamma}_i = \boldsymbol{\gamma}(\mathcal{S}_{h,p_i})\}_{i=1}^{N_P}$ is simple. $\hat{\Gamma} = \partial\hat{\Omega}$ can be parametrized with $\hat{\boldsymbol{\gamma}} = \mathcal{I}_h \boldsymbol{\gamma}$ where $\mathcal{I}_h$ denotes the linear Lagrange interpolation operator with respect to the triangulation $\mathcal{S}_h$.
3. $\{\boldsymbol{\gamma}_i\}_{i=1}^{N_P}$ contains all points where Γ is not C^{k+2}.
4. $\mathcal{S}_h$ consists of N triangles $Ŧ_i$ with vertices $\{Ŧ_{i,j}\}_{j=1}^{3}$, $i = 1, ..., N$.

Now, let $\hat{\mathcal{T}}_h$ denote a quasi-uniform triangulation (consisting of $\bar{N}$ tetrahedra) of $\hat{\Omega}$ such that the boundary points of $\hat{\mathcal{T}}_h$ are given with $\{\boldsymbol{\gamma}_i\}_{i=1}^{N_P}$. For $i \leqslant N$, let $\hat{T}_i$ denote the tetrahedron of $\hat{\mathcal{T}}_h$ whose intersection with $\hat{\Gamma}$ is the triangle $\hat{\boldsymbol{\gamma}}(Ŧ_i)$. For $i > N$, the intersection of the tetrahedron $\hat{T}_i$ with $\hat{\Gamma}$ is not necessary a unique point, as it can be a whole edge of $\hat{\boldsymbol{\gamma}}(Ŧ_i)$, see Figure 2. Assume that the tetrahedra are numbered such that $\dim\,(\hat{T}_i \cap \hat{\Gamma}) = 1$ if and only if $N < i \leqslant \mathring{N}$.

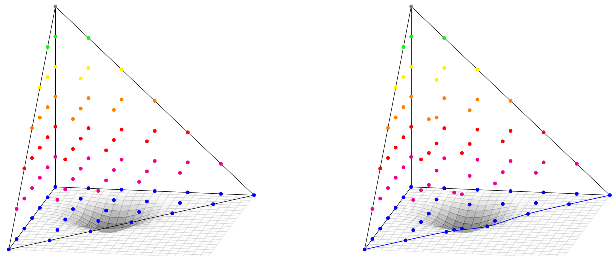

Fig. 2.2. *Example of the stretching resulting from* $\mathbf{Z}_i^2,\ i \leqslant N$

The further steps imply the reference tetrahedron

$$\hat{T}_{ref} = \left\{ \mathbf{x} = (x_1, x_2, x_3) \in \mathbb{R}^3 \ : \ x_i \geqslant 0 \text{ and } \sum_{i=0}^{3} x_i \leqslant 1 \right\} \tag{2.2}$$

and the reference transformation $\mathbf{F}_{\mathrm{ref},\hat{T}_i} : \hat{T}_i \to T_{\mathrm{ref}}$ such that

$$\mathbf{F}_{\mathrm{ref},\hat{T}_i}(\hat{T}_i \cap \hat{\Gamma}) = \begin{cases} F_{\mathrm{ref}} = \{(x_1,x_2,0) \ : \ 0 \leqslant x_1 \leqslant 1, 0 \leqslant x_2 \leqslant 1 - x_1\} & i \leqslant N \\ E_{\mathrm{ref}} = \{(x_1,0,0) \ : \ 0 \leqslant x_1 \leqslant 1\} & N < i \leqslant \mathring{N} \end{cases} \tag{2.3}$$

holds. Moreover, the following notation is introduced:

- For $i \leqslant N$, $\mathscr{V}_3(\hat{T}_i)$ denotes the vertex of $\hat{T}_i$ whose intersection with $\hat{\boldsymbol{\gamma}}(\mathcal{F}_i)$ is empty.
- $\mathscr{V}_3(\hat{T}_{\mathrm{ref}}) = (0, 0, 1)$.
- For $i \leqslant N$, $F_i = \hat{\boldsymbol{\gamma}}(\mathcal{F})$ is the triangle with the vertices $\{\boldsymbol{\gamma}(\mathcal{F}_{i,j})\}_{j=1}^3$ and $\widetilde{F}_i = \boldsymbol{\gamma}(\mathcal{F}_i)$ denotes the corresponding curved triangle on Γ_i.
- For $N < i \leqslant \mathring{N}$, E_i denotes the edge $\hat{T}_i \cap \hat{\Gamma}_i$ and $\widetilde{E}_i = \boldsymbol{\gamma}(E_i)$.
- For $N < i \leqslant \mathring{N}$, $\bar{E}_i$ denotes the edge of $\hat{T}_i$ whose intersection with E_i is empty.
- $\bar{E}_{\mathrm{ref}} = \{(0, t, 1-t) \ : \ t \in [0, 1]\}$.

Figure 2 summarizes these notations. Replacing the boundary triangle F_i of $\hat{T}_i$ by the curved triangle $\widetilde{F}_i$ leads to a curved tetrahedron $\widetilde{T}_i$ for $i \leqslant N$. For $N < i \leqslant \mathring{N}$, the curved tetrahedron $\widetilde{T}_i$ is obtained by replacing the edge E_i by the curved one $\widetilde{E}_i$. For $i \leqslant N$, the construction of the mapping $\hat{\mathbf{\Phi}}_h : \hat{T}_i \to \widetilde{T}_i$ can be reduced to the two-dimensional case. It involves a mapping $\mathbf{Z}^2$ that connects an interior point with a corresponding point on the approximated boundary. Therefore, the mapping $\mathbf{Z}^2_{\mathrm{ref}}$ to connect an interior point with a corresponding point on the edge F_{ref} is needed first. For a point $\mathbf{x}_{\mathrm{ref}} = (x_{\mathrm{ref}}, y_{\mathrm{ref}}, z_{\mathrm{ref}}) \in \hat{T}_{\mathrm{ref}}$ consider the line from $(0, 0, 1)$ through the point $\mathbf{x}_{\mathrm{ref}}$. As it crosses the face F_{ref}

at the point $\left(-\frac{x_{\text{ref}}}{z_{\text{ref}}-1}, -\frac{y_{\text{ref}}}{z_{\text{ref}}-1}, 0\right)$ the mapping $\mathbf{Z}_{\text{ref}}$ is defined as follows:

$$\begin{aligned} \mathbf{Z}^2_{\text{ref}} \ : \ \hat{T}_{\text{ref}} \to & \qquad F_{\text{ref}} \\ \mathbf{x}_{\text{ref}} \mapsto & \qquad \left(\frac{x_{\text{ref}}}{1-z_{\text{ref}}}, \frac{y_{\text{ref}}}{1-z_{\text{ref}}}, 0\right). \end{aligned}$$

With this mapping $\mathbf{Z}^2_{\text{ref}}$, a mapping $\mathbf{Z}^2_i = \mathbf{F}_{\text{ref},\hat{T}_i} \circ \mathbf{Z}^2_{\text{ref}} \circ \mathbf{F}^{-1}_{\text{ref},\hat{T}_i}$ can be defined to connect an interior point of any tetrahedron $\hat{T}_i$ with a corresponding point on $\hat{\Gamma}_i$. Note that any point $\mathbf{x} \in \hat{T}_i$ is located on the line segment $[\mathscr{V}_3(\hat{T}_i), \mathbf{Z}^2_i(\mathbf{x})]$ and the position of $\mathbf{x}$ on this line can be given with the ratio $\delta(\mathbf{x})$ of the distance between $\mathscr{V}_3(\hat{T}_i)$ and $\mathbf{x}$ to the distance between $\mathscr{V}_3(\hat{T}_i)$ and $\mathbf{Z}^2_i(\mathbf{x})$, i.e.:

$$\delta(\mathbf{x}) = \frac{\operatorname{dist}(\mathscr{V}_3(\hat{T}_i), \mathbf{x})}{\operatorname{dist}(\mathscr{V}_3(\hat{T}_i), \mathbf{Z}^2_i(\mathbf{x}))}. \tag{2.4}$$

Note that due to the fact that the affine mapping conserves the ratio of the distances, it holds

$$\delta(\mathbf{x}) = \frac{\operatorname{dist}\left((0,0,1), \mathbf{F}^{-1}_{\text{ref},\hat{T}_i}(\mathbf{x})\right)}{\operatorname{dist}\left((0,0,1), \mathbf{Z}^2_{\text{ref}}(\mathbf{F}^{-1}_{\text{ref},\hat{T}_i}(\mathbf{x}))\right)}. \tag{2.5}$$

The next step in the construction of $\hat{\mathbf{\Phi}}_h$ is to connect $\mathbf{Z}^2_i(\mathbf{x})$ to a point on Γ_i and therefore, map the point $\mathbf{Z}_i(\mathbf{x})$ back onto the domain of the chart with $\hat{\boldsymbol{\gamma}}$. As $\hat{\boldsymbol{\gamma}}$ is invertible, define $\hat{\boldsymbol{\zeta}} = \boldsymbol{\gamma} \circ \hat{\boldsymbol{\gamma}}^{-1}$, such that $\hat{\boldsymbol{\zeta}}$ maps $\hat{\Gamma}$ on Γ. Then, the point $\hat{\boldsymbol{\zeta}}(\mathbf{Z}^2(\mathbf{x}))$ has to be mapped back onto the interior of the tetrahedron. As the mapping $\hat{\mathbf{\Phi}}_{h,i} = \hat{\mathbf{\Phi}}_{h|_{\hat{T}_i}}$ has to be the identity map on the faces of $\hat{T}_i$ that are not mapped on the curved boundary, the point $\hat{\boldsymbol{\zeta}}(\mathbf{z}(\mathbf{x}))$ has to be mapped back to the line thought the fourth point of the tetrahedron, and such that the ratio of the distance between $\mathscr{V}_3(\hat{T}_i)$ and $\hat{\boldsymbol{\zeta}}(\mathbf{Z}_i(\mathbf{x}))$ to the distance between $\mathscr{V}_3(\hat{T}_i)$ and the mapped back point is equal to $\delta(\mathbf{x})$. This is illustrated in Figures 2.2 and 2.3. Let $\mathbf{Y}^2_{i,\delta} : \Gamma_i \to \widetilde{T}_i$ denote this mapping:

$$\mathbf{Y}^2_{i,\delta} = \mathbf{F}^{-1}_{\text{ref},\hat{T}_i} \circ \mathbf{Y}^2_{\text{ref},\delta} \circ \mathbf{F}_{\text{ref},\hat{T}_i} \tag{2.6}$$

where

$$\begin{aligned} \mathbf{Y}^2_{\text{ref},\delta} &: \mathbb{R}^3 \to \mathbb{R}^3 \\ &(x,y,z) \mapsto (x\delta, y\delta, z\delta + 1 - \delta) \ . \end{aligned} \tag{2.7}$$

Now, the mapping $\hat{\mathbf{\Phi}}_{h,i}$ can be defined as

$$\hat{\mathbf{\Phi}}_{h,i}(\mathbf{x}) = \mathbf{Y}^2_{i,\delta(\mathbf{x})}(\hat{\boldsymbol{\zeta}}(\mathbf{Z}^2_i(\mathbf{x}))), \ i \leqslant N. \tag{2.8}$$

For $N < i \leqslant \mathring{N}$ the point $\mathbf{x}$ on the interior of $\hat{T}_i$ has to be mapped onto E_i. This can be done considering the plane formed by $\mathbf{x}$ and $\bar{E}_i$ and choosing the unique intersection point with E_i, such that on each face of $\hat{T}_i$ whose intersection with

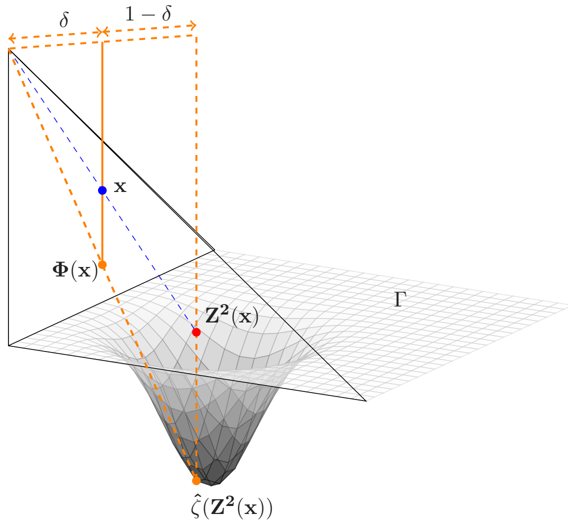

Fig. 2.3. *Construction of the mapping* $\hat{\mathbf{\Phi}}_i,\ i \leqslant N$

Γ_i is E_i, this mapping is identical to $\mathbf{Z}^2$. This leads to

$$\begin{aligned} \mathbf{Z}^1_{\text{ref}} \ :\ \hat{T}_{\text{ref}} \to &\quad E_{\text{ref}} \\ \mathbf{x}_{\text{ref}} \mapsto &\quad \begin{cases} \left(-\dfrac{x_{\text{ref}}}{z_{\text{ref}}+y_{\text{ref}}-1}, 0, 0\right) & \mathbf{x} \notin \bar{E}_{\text{ref}} \\ \mathbf{x} & \mathbf{x} \in \bar{E}_{\text{ref}}. \end{cases} \end{aligned}$$

Similarly to the case $i \leqslant N$, define $\mathbf{Z}^1_i = \mathbf{F}_{\text{ref},\hat{T}_i} \circ \mathbf{Z}^1_{\text{ref}} \circ \mathbf{F}^{-1}_{\text{ref},\hat{T}_i}$. Then, the point $\hat{\boldsymbol{\zeta}}(\mathbf{Z}^1(\mathbf{x}))$ has to be mapped back onto the interior of the tetrahedron. Consider that the mapping $\hat{\mathbf{\Phi}}_{h,i}$ has to be the identity on the two faces of $\hat{T}_i$ whose intersection with $\hat{\Gamma}_i$ is not E_i and that it has to be identical with $\mathbf{Z}^2$ on the two other faces. This means that the barycentric coordinates of $\hat{\mathbf{\Phi}}(\mathbf{x})$ in the triangle formed with $\bar{E}_i$ and $\hat{\boldsymbol{\zeta}}(\mathbf{Z}^1(\mathbf{x}))$ have to be identical to the barycentric coordinates of $\mathbf{x}$ in the triangle formed with $\bar{E}_i$ and $\mathbf{Z}^1(\mathbf{x})$. Let (δ_1, δ_2) denote these barycentric coordinates. Then,

$$\begin{aligned} \mathbf{Y}^1_{\text{ref},\delta_1,\delta_2} &: \mathbb{R}^3 \to \mathbb{R}^3 \\ &(x,y,z) \mapsto ((1-\delta_1-\delta_2)x, \delta_1 + y - \delta_1 y - \delta_2 y, \delta_2 + z - \delta_1 z - \delta_2 z)) \end{aligned} \tag{2.9}$$

maps a point $\mathbf{x}$ of $\mathbb{R}^3$ onto a point in the triangle formed by $\bar{E}_{\text{ref}}$ and $\mathbf{x}$ at the barycentric coordinates (δ_1, δ_2). Note that the barycentric coordinates of $\mathbf{x}_{\text{ref}}$ in the triangle formed with $\bar{E}_{\text{ref}}$ and $\mathbf{Z}^1_{\text{ref}}(\mathbf{x}_)$ are given by $(y_{\text{ref}}, z_{\text{ref}})$ such that

$$\hat{\mathbf{\Phi}}_{h,\text{ref}}(\mathbf{x}) = \mathbf{Y}^1_{\text{ref},y,z}(\hat{\boldsymbol{\zeta}}(\mathbf{Z}^1_{\text{ref}}(\mathbf{x}))) \tag{2.10}$$

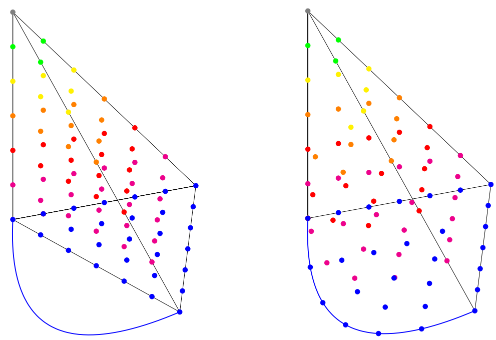

Fig. 2.4. *Example of the stretching resulting from* $\mathbf{Z}_i^1,\ N < i \leqslant \mathring{N}$

maps $\hat{T}_{\mathrm{ref}}$ onto $\widetilde{T}_{\mathrm{ref}}$. Using the transformation $\mathbf{F}_{\mathrm{ref},\hat{T}_i}$ leads to

$$\hat{\mathbf{\Phi}}_{h,i} = \mathbf{F}_{\mathrm{ref},\hat{T}_i} \circ \hat{\mathbf{\Phi}}_{h,\mathrm{ref}}(\mathbf{x}) \circ \mathbf{F}^{-1}_{\mathrm{ref},\hat{T}_i} \; . \tag{2.11}$$

This construction is illustrated in Figures 2.4 and 2.5. Setting $\hat{\mathbf{\Phi}}_{h,i} = \mathrm{id}$ for the interior elements leads to the global definition of $\hat{\mathbf{\Phi}}_h$. This construction reduced to a well-known polygonal interpolation and leads to the following properties (see [4]).

LEMMA 2.1.
With the previous assumptions and $\hat{T}_i \in \hat{\mathcal{T}}_h$, $\hat{\mathbf{\Phi}}_{h,i}$ is a $\mathcal{C}^2$ diffeomorphism and it holds

$$\|\hat{\mathbf{\Phi}}_{h,i} - \mathrm{id}\|_{W^j_\infty(\hat{T}_i)} \lesssim h^{2-j} \quad \forall j \leqslant 2 \tag{2.12}$$

$$\|\det(J_{\hat{\mathbf{\Phi}}_{h,i}}) - 1\|_{\infty,\hat{T}_i} \lesssim h. \tag{2.13}$$

Moreover, $J_{\hat{\mathbf{\Phi}}_{h,i}}$ is invertible and $\hat{\mathbf{\Phi}}_{h,i} : \hat{T}_i \to \widetilde{T}_i$ is injective. The mapping $\hat{\mathbf{\Psi}}_{h,i} = \hat{\mathbf{\Phi}}^{-1}_{h,i}$ satisfies

$$\begin{aligned} \|\hat{\mathbf{\Psi}}_{h,i} - \mathrm{id}\|_{W^j_\infty(\widetilde{T}_i)} &\lesssim h^{2-j} \quad \forall j \leqslant 2 \\ \|\det(J_{\hat{\mathbf{\Psi}}_{h,i}}) - 1\|_{\infty,\widetilde{T}_i} &\lesssim h. \end{aligned} \tag{2.14}$$

For the construction of an approximated domain Ω_h with piecewise polynomial boundary, consider that the two-dimensional Lagrangian elements can be defined on the triangulation $\mathcal{S}_h$. Recall that the degrees of freedom are given by

$$\mathcal{N} = \Big\{ \boldsymbol{\gamma}(\mathcal{T}_{i,l}) + \sum_{j=1}^{2} \frac{\lambda_j}{k} \left(\boldsymbol{\gamma}(\mathcal{T}_{i,j}) - \boldsymbol{\gamma}(\mathcal{T}_{i,l}) \right) : 1 \leqslant l \leqslant 3,\ j \neq l, \lambda_j \in \mathbb{N}_0, \\ \lambda_1 + \lambda_2 \leqslant k \Big\} \tag{2.15}$$

for each $\mathcal{T}_i$ in $\mathcal{S}_h$. Using the interpolation operator $\mathcal{I}_h$ with respect to these nodal points leads to parametrization of the polynomial boundary $\gamma_h = \mathcal{I}_h \boldsymbol{\gamma}$. Let Ω_h denote the corresponding polynomial domain and $\Gamma_h = \partial\Omega_h = \{\gamma_h(\mathbf{x}) : \mathbf{x} \in D\}$. $F_h : \hat{\Omega} \to \Omega_h$ can be constructed using the same way as above for $\hat{\boldsymbol{\Phi}}_h$, replacing $\boldsymbol{\gamma}$ by $\boldsymbol{\gamma}_h$, i.e. replacing $\hat{\boldsymbol{\zeta}}$ by $\boldsymbol{\zeta} = \boldsymbol{\gamma}_h \circ \hat{\boldsymbol{\gamma}}_h^{-1}$

$$F_{h,i} = \mathbf{F}_{\mathrm{ref},\hat{T}_i} \circ F_{h,\mathrm{ref},i}(\mathbf{x}) \circ \mathbf{F}^{-1}_{\mathrm{ref},\hat{T}_i} \tag{2.16}$$

with

$$F_{h,\mathrm{ref},i} = \begin{cases} \mathbf{Y}^2_{\mathrm{ref},\delta(\mathbf{x})}(\boldsymbol{\zeta}(\mathbf{Z}^2_{\mathrm{ref}}(\mathbf{x}))) & i \leqslant N \\ \mathbf{Y}^1_{\mathrm{ref},y,z}(\boldsymbol{\zeta}(\mathbf{Z}^1_{\mathrm{ref}}(\mathbf{x}))) & N < i \leqslant \mathring{N} \\ id & i > \mathring{N} \end{cases} . \tag{2.17}$$

Similarly to the construction of $\hat{\boldsymbol{\Phi}}$, this construction leads to the following properties (see [4]). Combining this with the classical interpolation bounds leads to the following theorem (see [4], Theorem 1).

Theorem 2.2.

With the previous assumptions and $\hat{T}_i \in \hat{\mathcal{T}}_h$, $F_{h,i}$ is a $\mathcal{C}^{k+2}$ diffeomorphism, polynomial of degree $k+1$ and invertible in a neighborhood of $\hat{\Omega}$. Moreover, for a positive integer s with $s \leqslant k+2$, it holds

$$\|F_h\|_{W^s_\infty(\hat{T}_i)} \lesssim h^s, \ \|F_h^{-1}\|_{W^s_\infty(\hat{T}_i)} \lesssim h^{-s} . \tag{2.18}$$

Note that the invertibility of $F_{h,i}$ in a neighborhood of $\hat{\Omega}$ can be used by the definition of the finite-elements to extend it from Ω_h to Ω for small enough h.

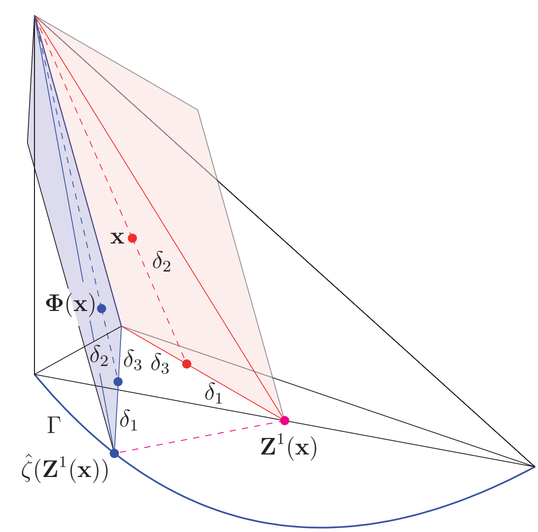

Fig. 2.5. *Construction of the mapping* $\hat{\boldsymbol{\Phi}}_i,\ N < i \leqslant \mathring{N}$

Further, an auxiliary mapping $\mathbf{\Phi}_h : \Omega_h \to \Omega$ can be given by $\mathbf{\Phi}_h = \hat{\mathbf{\Phi}}_h \circ F_h^{-1}$. Combining the properties from $\hat{\mathbf{\Phi}}_h$ and F_h leads to the following theorem (see [4], Paragraph 5):

THEOREM 2.3.
With the previous assumptions and $\hat{T}_i \in \hat{\mathcal{T}}_h$, $\mathbf{\Phi}_{h,i}$ is a $\mathcal{C}^{k+2}$ diffeomorphism and for a positive integer with $s \leqslant k+2$, it holds

$$\|\mathbf{\Phi} - id\|_{W^s_\infty(T_i)} \lesssim h^{k+2-s} \tag{2.19}$$

$$\text{and } \|\det(J_{\mathbf{\Phi}_{i,h}}) - 1\|_{L^\infty(T_i)} \lesssim h^{k+1} \tag{2.20}$$

Further, the mapping $\mathbf{\Phi}_{h,i} : T_i \to \widetilde{T}_i$ is injective and $\mathbf{\Psi}_{h,i} = \mathbf{\Phi}_{h,i}^{-1}$ satisfies

$$\|\mathbf{\Psi} - id\|_{W^s_\infty(\widetilde{T}_i)} \lesssim h^{k+2-s} \quad \forall s \leqslant k+2 \tag{2.21}$$

$$\text{and } \|\det(J_{\mathbf{\Psi}_{i,h}}) - 1\|_{L^\infty(\widetilde{T}_i)} \lesssim h^{k+1} \tag{2.22}$$

Proof 2.4 *Note that $\mathbf{\Phi}_{h,i}$ is the identity mapping on the two edges of T_i which have one single common point with Γ_h. Further, due to its construction it holds*

$$\mathbf{\Phi}_h \circ \boldsymbol{\gamma}_h = \boldsymbol{\gamma} \tag{2.23}$$

and

$$\begin{aligned}
\mathbf{\Phi}_{h,i}(\mathbf{x}) - \mathbf{x} &= \mathbf{Y}_{\delta(F_{h,i}^{-1}(\mathbf{x}))}(\hat{\boldsymbol{\zeta}}(\boldsymbol{\zeta}^{-1}(\mathbf{Y}^{-1}_{\delta(F_{h,i}^{-1}(\mathbf{x}))}))) - \mathbf{Y}_{\delta(F_{h,i}^{-1}(\mathbf{x}))}(\mathbf{Y}^{-1}_{\delta(F_{h,i}^{-1}(\mathbf{x}))}) \\
&= \mathbf{Y}_{\delta(F_{h,i}^{-1}(\mathbf{x}))}((\boldsymbol{\gamma} \circ \boldsymbol{\gamma}_h^{-1} - \boldsymbol{\gamma}_h \circ \boldsymbol{\gamma}_h^{-1})(\mathbf{Y}^{-1}_{\delta(F_{h,i}^{-1}(\mathbf{x}))})) \\
&= \mathbf{Y}_{\delta(F_{h,i}^{-1}(\mathbf{x}))}(((\boldsymbol{\gamma} - \boldsymbol{\gamma}_h) \circ \boldsymbol{\gamma}_h^{-1})(\mathbf{Y}^{-1}_{\delta(F_{h,i}^{-1}(\mathbf{x}))}))
\end{aligned}$$

such that the further steps consist in using the classical interpolation theory and the smoothness properties of $\mathbf{Y}$ and $\boldsymbol{\gamma}_h^{-1}$.

3. A theoretical example

A simple example is given considering a two-phase stokes flow, where the domain, $\Omega \subset \mathbb{R}^2$, is assumed to be completely covered by Ω_1 and Ω_2 with $\Omega_1 \subset \Omega_2$ and Γ denotes the boundary of Ω_1 as illustrated in Figure 3.1. Let $\mathbf{n}$ be the unit normal on Γ that is pointing from Ω_1 to Ω_2 and κ denote the curvature of Γ. Assuming that no phase transition takes place and that the two phases are viscous, the two-phase model reduces to governing equations in each phase and coupling conditions at the interface. In order to keep the problem as simple as possible, consider the stationary Stokes equations of Newtonian fluids such that for the stress tensor, $\boldsymbol{\sigma}_{\Omega_i}$, it holds $\boldsymbol{\sigma}_{\Omega_i} = -p_{\Omega_i}\mathbf{I} + \mu_i \mathbf{D}(\mathbf{u})$ in each phase Ω_i, with a constant dynamic viscosity $\mu_i > 0$ and the deformation tensor $\mathbf{D}(\mathbf{u}) = \nabla\mathbf{u} + (\nabla\mathbf{u})^\top$. The velocity $\mathbf{u}$ is continuous over the whole domain Ω, i.e., in the context of variational formulations $\mathbf{u}$ is searched in $H^1(\Omega)$. In opposition to the velocity, the pressure is discontinuous over the interface. Therefore $p_{\Omega_i} \in H^2(\Omega_i)$ denotes the pressure in each phase Ω_i.

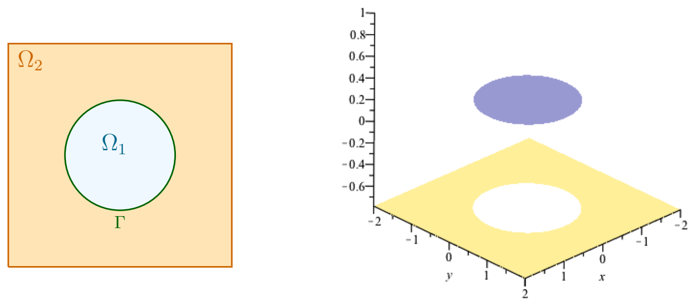

Fig. 3.1. *Exact pressure for the rotational flow* $\mathbf{u}(\mathbf{x}) = (-y, x)$

However, in order to simplify the notation the index i is skipped whenever the restriction on each phase is not needed. Due to the fact that on both sides of Γ there are different molecules with different attractive forces, a surface tension force acts at the interface, and this leads to the coupling condition

$$(\boldsymbol{\sigma}_{\Omega_2} - \boldsymbol{\sigma}_{\Omega_1}) \cdot \mathbf{n} = -\tau\kappa\mathbf{n} \text{ on } \Gamma \ , \tag{3.1}$$

where τ denotes the constant surface tension coefficient. The first-order system formulation reads:

$$\left.\begin{aligned} \operatorname{div} \boldsymbol{\sigma}_{\Omega_i} &= \mathbf{0} \\ \operatorname{dev} \boldsymbol{\sigma} - \mu_i \mathbf{D}(\mathbf{u}) &= \mathbf{0} \end{aligned}\right\} \quad \text{in } \Omega,\ i = 1, 2,$$
$$\begin{aligned} (\boldsymbol{\sigma}_{\Omega_2} - \boldsymbol{\sigma}_{\Omega_1}) &= -\kappa\mathbf{n} \qquad \text{on } \Gamma \\ (\operatorname{tr} \ \boldsymbol{\sigma}, 1)_\Omega &= 0, \end{aligned} \tag{3.2}$$

where $\operatorname{dev} \mathbf{A}$ means the deviator of $\mathbf{A}$ defined by

$$\operatorname{dev}\mathbf{A} := \mathbf{A} - \frac{1}{n}\operatorname{tr}(\mathbf{A})I, \quad \text{for} \ \ \mathbf{A} \in \mathbb{R}^{n\times n}.$$

The least squares functional associated with the problem (3.2) is

$$\mathcal{F}(\boldsymbol{\sigma}, \mathbf{u}) = \sum_{i=1}^{2} \| \frac{1}{\sqrt{\mu_i}} \operatorname{dev} \boldsymbol{\sigma} - \sqrt{\mu_i}\ \mathbf{D}(\mathbf{u}) \|^2_{0,\Omega_i} + \|\operatorname{div} \boldsymbol{\sigma}_{\Omega_i}\|^2_{0,\Omega_i} \tag{3.3}$$

for $\mathbf{u} \in \mathcal{W} = \left(H^1_0(\Omega)\right)^2$ and

$$\begin{aligned} \boldsymbol{\sigma} \in \boldsymbol{\Sigma} = \{\boldsymbol{\sigma} = (\boldsymbol{\sigma}_{\Omega_1}, \boldsymbol{\sigma}_{\Omega_2}) \ : \boldsymbol{\sigma}_{\Omega_i} \in (H(\operatorname{div}, \Omega_i))^2, \ i = 1, 2,& \\ (\boldsymbol{\sigma}_{\Omega_2} - \boldsymbol{\sigma}_{\Omega_1}) \cdot \mathbf{n} = -\kappa\mathbf{n} \text{ on } \Gamma& \\ \text{and } (\operatorname{tr} \ \boldsymbol{\sigma}, 1)_{0,\Omega} = 0\} \ .& \end{aligned} \tag{3.4}$$

In order to simplify the notation, $[\boldsymbol{\sigma} \cdot \mathbf{n}]_\Gamma$ denotes the jump $(\boldsymbol{\sigma}_{\Omega,2} - \boldsymbol{\sigma}_{\Omega,1}) \cdot \mathbf{n}$ over Γ. For a rotational flow $\mathbf{u}(\mathbf{x}) = (-y, x)$ in a two-phase domain with a unit circular interface (see e.g. [3]), it implies $\mathbf{D}(\mathbf{u}) = 0$ and thus, the deviator of the stress tensor is zero. Due to the fact that in each phase, the stress tensor is divergence-free as well, this implies $\boldsymbol{\sigma}_{\Omega_i} = \alpha_i \mathbf{I}$ for constants α_i. Then, the interface condition leads to $\alpha_2 = -\kappa + \alpha_1 = -1 + \alpha_1$. Considering the normalizing condition $(\mathrm{tr}\ \boldsymbol{\sigma}, 1)_\Omega = 0$ leads to

$$\alpha_1 |\Omega_1| + \alpha_2 |\Omega_2| = 0 \tag{3.5}$$

and thus to the following exact solution, that only depends on the surface of the domains Ω_i.

$$\boldsymbol{\sigma}_{\Omega_1} = \frac{|\Omega_2|}{|\Omega|}\mathbf{I} \tag{3.6}$$

$$\boldsymbol{\sigma}_{\Omega_2} = -\frac{|\Omega_1|}{|\Omega|}\mathbf{I}. \tag{3.7}$$

The corresponding pressure $p_i = \mathrm{tr}\ \boldsymbol{\sigma}_i = 2\alpha_i$ is shown for $\Omega_2 = [-2,2]\times[-2,2]$ in Figure 3.1. This solution belongs to the standard conforming finite element space for $\mathcal{W}\times\boldsymbol{\Sigma}$, i.e., a Raviart-Thomas space of degree k combined with $\mathcal{P}_{k+1}$ subject to the appropriate boundary and interface conditions. Hence, only the approximation of the domain leads to an approximation of the solution. The numerical computation leads to the solution

$$\boldsymbol{\sigma}_{\Omega_{h,1}} = -\frac{|\Omega_{h,2}|}{|\Omega|}, \qquad \boldsymbol{\sigma}_{\Omega_{h,2}} = \frac{|\Omega_{h,1}|}{|\Omega|}. \tag{3.8}$$

This is as good as the approximation of the domain. In particular, this clearly demonstrates that a polygonal approximation of the boundary is not sufficient to retain the optimal convergence order in the higher-order case.

Bibliography

[1] F. BERTRAND, S. MÜNZENMAIER, and G. STARKE, First-order system least squares on curved boundaries: Lowest-order Raviart-Thomas elements, SIAM Journal on Numerical Analysis 52 (2014) (2) : 880-894.

[2] F. BERTRAND, S. MÜNZENMAIER, and G. STARKE, First-order system least squares on curved boundaries: Higher-order Raviart-Thomas elements, SIAM Journal on Numerical Analysis, 52 (6), 3165-3180.

[3] S. GANESAN, G. MATTHIES AND L. TOBISKA, On spurious velocities in incompressible flow problems with interfaces, Computer Methods in Applied Mechanics and Engineering 196(7): 1193-1202, 2007.

[4] M. LENOIR, Optimal isoparametric finite elements and error estimates for domains involving curved boundaries, SIAM Journal on Numerical Analysis, (1986), 23:562–58..

[5] P. J. MATUSZYK and L. F. DEMKOWICZ, Parametric finite elements, exact sequences and perfectly matched layers, Computational Mechanics, 51 (2013), 35-45.

[6] M. E. ROGNES, R. C. KIRBY, and A. LOGG, Efficient assembly of H(div) and H(curl) conforming finite elements, SIAM Journal on Scientific Computing, 31 (2009) 4130-4151.

Colloque Fédération Normandie-Mathématiques

EDP - Normandie

21 & 22 Octobre 2015

Université du Havre
Laboratoire de Mathématiques Appliquées du Havre
UFR des Sciences et Techniques

COMITÉ SCIENTIFIQUE

Laurent Boudin (LJLL, UPMC & Reo, Inria)
Catherine Choquet (MIA, La Rochelle)
Rabah Labbas (LMAH, Le Havre)
Annie Raoult (MAP5, Paris Descartes)
Taoufik Sassi (LMNO, Caen)

COMITÉ D'ORGANISATION

Benjamin Ambrosio (LMAH, Le Havre)
Christian Dogbe (LMNO, Caen)
Valentina Lanza (LMAH, Le Havre)
Mohammed Louaked (LMNO, Caen)
Sorin Mardaré (LMRS, Rouen)

Université du Havre
Laboratoire de Mathématiques
Appliquées du Havre
UFR des Sciences et Techniques
25, rue Philippe Lebon - BP 540
76058 - LE HAVRE

Fédération
Normandie-Mathématiques
FR CNRS 3335

CONFÉRENCIERS

Farid Ammar Khodja (Besançon)
Dwight Barkley (Warwick)
Ariela Briani (Tours)
Paola Causin (Milan)
Philippe G. Ciarlet (Hong Kong)
Michel Chipot (Zurich)
Stephen Coombes (Nottingham)
Isabelle Gallagher (Paris)
Kamel Hamdache (Paris)
François Hamel (Aix-Marseille)
Petru Mironescu (Lyon)
Olivier Pantz (Polytechnique)
Benoit Perthame (Paris)
Delphine Salort (Paris)
Nicoletta Tchou (Rennes)
Hatem Zaag (Paris)

Site Web: http://edp-normandie3.sciencesconf.org/
Blog: http://edp-normandie3.blogspot.fr/
Email: edp-normandie3@sciencesconf.org

Fiche d'inscription sur le site WEB de la conférence
Date limite d'inscription : 12 Octobre 2015

Image en arrière plan : "Entrée du port du Havre" de Léon Auguste Asselineau (1808-1889)

Actes des Colloques “EDP-Normandie”

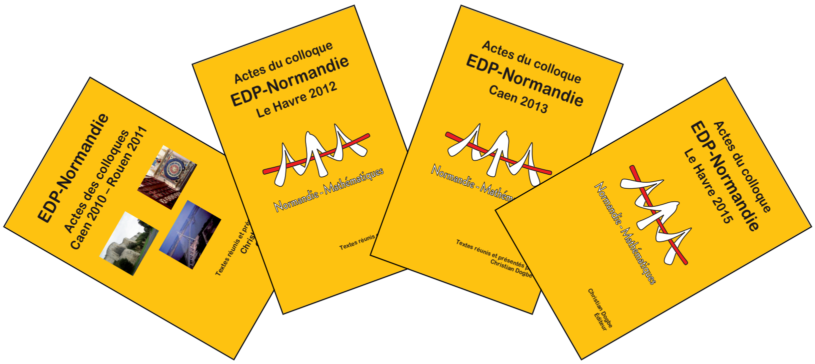

- **Actes des colloques Caen 2010 - Rouen 2011**
  39+33 communications, 362 pages.
  ISBN 978-2-9541221-0-6
- **Actes du colloque Le Havre 2012**
  14 communications, 150 pages.
  ISBN 978-2-9541221-1-3
- **Actes du colloque Caen 2013**
  17 communications et 26 posters, 350 pages.
  ISBN 978-2-9541221-2-0
- **Actes du colloque Le Havre 2015**
  20 communications et 40 posters, 432 pages.
  ISBN 978-2-9541221-3-7

Département de mathématiques et mécanique

Campus 2, Côte de Nacre
Boulevard Maréchal Juin
Bâtiment Sciences 3
Bureaux S3-206/213
14 032 Caen CEDEX
Tel. : 02 31 56 73 60
Fax : 02 31 56 73 20
sonia.esnault@unicaen.fr

Dogbe, Christian (ed.)

Proceedings of the 5th "EDP-Normandie" colloquium of the Fédération Normandie-Mathématiques on partial differential equations and its applications, Le Havre, France, October 21–22, 2015. (Actes du colloque "EDP-Normandie", Le Havre, France, Octobre 21–22, 2015.) (French, English) Zbl 06550722

Normandie-Mathématique. [s.l.]: Fédération Normandie-Mathématiques (ISBN 978-2-9541221-3-7/pbk). xxix, 396 p. (2016).

The articles of this volume will be reviewed individually. For the preceding colloquium see [Zbl 1296.35005].

MSC:

35-06 Proceedings of conferences (partial differential equations)
35Qxx PDE of mathematical physics and other areas
00B25 Proceedings of conferences of miscellaneous specific interest

zbMATH
the first resource for mathematics

Dogbe, Christian (ed.)

Proceedings of the 4th "EDP-Normandie" colloquium of the Fédération Normandie-Mathématiques on partial differential equations and its applications, Caen, France, October 24–25, 2013. (Actes du colloque "EDP-Normandie", Caen, France, Octobre 24–25, 2013.) (French, English) Zbl 1296.35005

Normandie-Mathématique. [s.l.]: Fédération Normandie-Mathématiques (ISBN 978-2-9541221-2-0/pbk). xxvi, 321 p. (2014).

The articles of this volume will be reviewed individually. For the preceding colloquium see [Zbl 1296.35006].

Indexed articles:

Amrouche, Chérif, Stokes and Navier-Stokes equations with different boundary conditions, 1-15 [Zbl 1311.35202]

Besse, Nicolas, Asymptotic analysis of the eigenvalue problem for the gyrowaterbag operator in toroidal geometry, 17-30 [Zbl 1327.35277]

Calvez, Vincent, Kinetic travelling waves with applications to biology, 31-41 [Zbl 1316.35068]

Esteban, Maria J., Spectral estimates on the sphere and on compact manifolds without boundary, 43-46 [Zbl 1316.58024]

Gerbeau, J-F.; Lombardi, D., Approximated Lax pairs and reduced order modeling, 47-53 [Zbl 06415589]

Lafitte, Pauline; Mascia, Corrado, Study of a transition phase model of nonlinear diffusion type, 55-61 [Zbl 1310.65111]

Maday, Yvon, Numerical analysis of some problems of electronic structure calculations, 63-64 [Zbl 1311.82046]

Mancini, Simona, On a Fokker-Planck equation modeling particles trapped in a double well potential, 65-73 [Zbl 1316.35285]

Monniaux, Sylvie, The Navier-Stokes system with Coriolis force in a halfspace with rough boundary, 75-86 [Zbl 06415593]

Aymard, B.; Clément, F.; Coquel, F.; Monniaux, D.; Postel, M., Numerical simulation of a hyperbolic PDE system with discontinuous flux, 87-99 [Zbl 1330.35462]

Salort, Delphine, Models of neuronal networks and synchronization phenomena, 101-113 [Zbl 1316.35288]

Turpault, R.; Berthon, C.; Boutin, B., Shock profiles for St-Venant-Exner, 115-124 [Zbl 1310.76084]

Nicolas, Vauchelet, Kinetic description and asymptotic models of bacteria motion in chemotaxis, 125-132 [Zbl 06415597]

Phan, V.L.Em; Ambrosio, B.; Aziz, M.A., Analysis of a complex and complete network of reaction-diffusion equations of FitzHugh-Nagumo type, 133-14 [Zbl 1325.35243]

Wilk, Olivier, Absorbing boundary conditions of high order, domain decomposition and wave models, 145-156 [Zbl 1311.76086]

Alberdi Celaya, E.; Anzala Aguirrezabala, J.J., The computation of EBDF and MEBDF methods using backward differences, 157-170 [Zbl 1310.65078]

Ambrosio, Benjamin, Hopf bifurcation for a reaction-diffusion system from neuroscience, 171-180 [Zbl 1311.35018]

Aguillon, Nina, A reconstruction schema in gas dynamics, 184-187 [Zbl 1310.76103]

Alberdi Celaya, E.; Anza Aguirrezabala, J.J., The behaviour of backward differentiation formulae in high-frequency modes, 190-191 [Zbl 1310.65116]

Bourdin, Loïc; Trélat, Emmanuel, The Pontryagin maximum principle for finite dimensional nonlinear optimal control problems on time scales, 198-202 [Zbl 1311.49049]

Boutarene, Khaled El-Ghaouti, Approximate transmission conditions for a Poisson problem, 206-208 [Zbl 1312.35062]

Breteaux, Sébastien, A geometric derivation of the linear Boltzmann equation, 212-213 [Zbl 1328.35140]

Cazeaux, Paul; Grandmont, Céline, A nonlocal homogenization model for the mechanical behavior of human lungs, 216-217 [Zbl 06415608]

Chatard, M.; Chainais-Hillairet, C.; Filbet, F., Discrete functional inequalities for finite volume schemes, 220-223 [Zbl 1312.65142]

Chourabi, Imen; Donato, Patrizia, A quasilinear singular problem with nonlinear Robin conditions, 226-228 [Zbl 1312.35063]

Cocquet, Pierre-Henri, A numerical scheme for approximation of metamaterial acoustics, 232-233 [Zbl 1311.74115]

Court, Sébastien, Stabilisation of a fluid-solid system, by the deformation of the self-propelled solid, 236-237 [Zbl 1311.35213]

Fouchet-Incaux, J.; Grandmont, C.; Martin, S., Modeling of the air flow in the human respiratory system: a numerical stability study, 240-241 [Zbl 1307.92058]

Gazeau, Maxime, Wave propagation in complex random environments, 244-245 [Zbl 1325.35295]

Lacouture, L.; Decoene, A.; Martin, S.; Maury, B., Numerical solution of elliptic problems with a Dirac mass on the right-hand side, 248-251 [Zbl 1311.76064]

Lahbib, Imen; Blouza, Adel, A posteriori analysis of an anisotropic shell of low regularity, 254-256 [Zbl 06415616]

Levitt, Antoine, Convergence of algorithms for Hartree-Fock models in quantum chemistry, 260-261 [Zbl 1315.81112]

Mimault, Matthias, Macroscopic modeling of crowd movements. An application to crowed decomposition into two groups, 264-271 [Zbl 1311.35154]

Boyer, Franck; Krell, Stella; Nabet, Flore, Inf-sup stability of DDFV schemes for the 2D Stokes problem, 274-279 [Zbl 1311.76077]

Najeme, Mohamed; Glangetas, Léo, Analytic and Gevrey regularity for kinetic equations, 282-283 [Zbl 1311.35046]

Phan, V.L.; Ambrosio, B.; Aziz-Alaoui, M., Complex networks of neurons modeled by PDEs of FitzHugh-Nagumo type, 286 [Zbl 1325.35242]

Rota Nodari, Simona, Study of a nonlinear model from nuclear physics, 290-292 [Zbl 1316.35267]

Runge, Vincent, Study of Hele-Shaw flow by Helmholtz-Kirchhoff transformation, 296-298 [Zbl 1311.35231]

Saleh, Khaled; Latché, Jean-Claude, A staggered scheme for the incompressible Navier-Stokes equations with variable density, 302-303 [Zbl 1311.35189]

Tine, Léon M.; Meunier, Nicolas, Mathematical modeling of atherosclerosis, 306-308 [Zbl 1311.35328]

Ali, Hani, Existence and convergence of a modified deconvolution model, 312-316 [Zbl 1311.35183]

Yvinec, Romain, Deterministic and stochastic nucleation models, 317-320 [Zbl 1311.35329]

MSC:

35-06 Proceedings of conferences (partial differential equations)
35Qxx PDE of mathematical physics and other areas
00B25 Proceedings of conferences of miscellaneous specific interest

Cited in **1** Review

Bon de commande

Actes des colloques de la collection
NORMANDIE-MATHEMATIQUES
(merci d'écrire en MAJUSCULE)

Normandie - Mathématiques

Nom :……………………………………………………………………………………………

Prénom :…………………………………………………………………………………………

Adresse :…………………………………………………………………………………….

……………………………………………………………………………………………………

Téléphone :…………………………………………………………………………………..

E.mail :………………………………………………………………………………………..

ISBN	Titres	Prix unitaire	Prix auteur	Quantité	Total
978-2-9541221-0-6	EDP-Normandie Actes des colloques Caen 2010 - Rouen 2011 (362 pages)	20 €	**15** €		
978-2-9541221-1-3	EDP-Normandie Actes du colloque Le Havre 2012 (150 pages)	15 €	**10** €		
978-2-9541221-2-0	EDP-Normandie Actes du colloque Caen 2013 (350 pages)	20 €	**15** €		
978-2-9541221-3-7	EDP-Normandie Actes du colloque Le Havre 2015 (432 pages)	25 €	**20** €		
	Les QUATRE volumes	70 €	**54** €		
	Participation aux frais de port*				
	Total à Payer				

* Participation aux frais de port :
- Pour toute commande inférieure à 25 € --> 2,80 €
- Pour toute commande entre 25 – 35 € --> 5,60 €
- Pour toute commande supérieure à 45 € --> frais de port offerts.

A …………………… Date de commande …………………………

Signature :

Bon de commande à retourner, accompagné de votre chèque à l'ordre de
l'agent comptable de l'université de Caen-Normandie, à l'adresse suivante :
Madame **Sonia Esnault**
Université de Caen-Normandie Département de Mathématiques Campus 2,
Côte de Nacre, Bd Maréchal Juin, 14032 Caen Cedex (France)
Téléphone : 02 31 56 73 60 Fax : 02 31 56 73 20 Courriel : **sonia.esnault@unicaen.fr**
Votre commande sera expédiée accompagnée d'une facture acquittée, dans les deux jours ouvrés qui suivront l'encaissement validé de votre règlement. *Merci et à bientôt !*